Thermodynamic and experimental investigations on the growth of thick aluminum nitride layers by high temperature CVD

A. Claudel, E. Blanquet, D. Chaussende, M. Audier, D. Pique, M. Pons

Thermodynamic and experimental investigations on the growth of thick aluminum nitride layers by high temperature CVD

A. Claudel [a,c,*], E. Blanquet [a], D. Chaussende [b], M. Audier [b], D. Pique [c], M. Pons [a]

[a] *Science et Ingénierie des Matériaux et des Procédés, Grenoble INP-CNRS-UJF, BP 75, 38402 Saint Martin D'Hères, France*
[b] *Laboratoire des Matériaux et du Génie Physique, Grenoble INP-CNRS, 3 parvis Louis Néel, BP 257, 38016 Grenoble, France*
[c] *ACERDE, 452 rue des sources, 38920 Crolles, France*

To achieve AlN bulk growth, high temperature CVD process using chlorine chemistry was investigated. High growth rate and high crystalline quality are targeted for both polycrystalline and epitaxial AlN films grown on (0 0 0 1) α-Al_2O_3 Sapphire and (0 0 0 1) off axis 4H SiC or on axis 6H SiC single crystal substrates. Thermodynamic calculations were carried out to select the more appropriate inert materials for the reactor and to understand the chemistries of Al chlorination and AlN deposition steps. The reactants were ammonia (NH_3) and aluminum chlorides ($AlCl_x$) species formed *in situ* using chlorine gas (Cl_2) reaction with high purity Al wires. Deposition temperature was varying from 1100 to 1800 °C. Influences of temperature, total pressure, Cl_2 flow rate and carrier gas (Ar or H_2) on growth rate, surface morphology and crystalline state are presented. As results, films morphology is related to a variation of the thermodynamic supersaturation. As-grown AlN layers surface morphologies were studied by SEM, FEG-SEM and AFM. Crystalline state, crystallographic orientations and epitaxial relationships with substrates were obtained from $\theta/2\theta$ X-ray diffraction and X-ray pole figure, respectively. Growth rates up to 200 $\mu m\,h^{-1}$ have been reached for polycrystalline AlN layers.

1. Introduction

Aluminum nitride AlN is a wide bandgap III–V semiconductor material. AlN single crystal is expected to be a promising substrate material because of its wide direct bandgap (Eg = 6.2 eV), its high electrical resistivity (between 10^9 and $10^{13}\,\Omega\,cm$ at 300 K) and high thermal conductivity ($3.3\,W\,K^{-1}\,cm^{-1}$), its small difference in thermal expansion coefficient and small lattice mismatch with SiC and GaN. The availability of AlN single crystal substrates is expected for applications such as group III nitride optoelectronics blue and UV LEDs and LDs, high frequency and high power devices (high electron mobility transistors: HEMT) or surface acoustic waves (SAW) emitters and detectors.

To date, most of the works dedicated to AlN bulk crystal growth have implemented the powder sublimation method (PVT) [1–3]. In 1959, Renner [4] grew the first AlN layers by CVD. Then, AlN epitaxial layers were obtained by reaction between anhydrous aluminum chloride and ammonia in 1967 and 1968 [5,6] or by direct reaction of the adduct compound $AlCl_3.NH_3$ between 1970 and 1977 [7–9]. Since 1972, epitaxial growth of AlN on Sapphire and SiC substrates by a vapor phase epitaxy process using Al, HCl and NH_3 have been studied at temperature of about 1100 °C [10–28]. Since 2007, several studies have been investigated to increase AlN layers crystalline quality and growth rate by increasing deposition temperature [29–35]. MOCVD epitaxial growth using trimethyl aluminum (TMA) and NH_3 was also investigated at 1200 °C and AlN layers of high crystalline quality can be obtained but at low growth rate ($3\,\mu m\,h^{-1}$) [36,37]. In this

*Corresponding author at: Science et Ingénierie des Matériaux et des Procédés, Grenoble INP-CNRS-UJF, BP 75, 38402 Saint Martin D'Hères, France.
Tel.: +33 476826530; fax: +33 476826677.
E-mail address: arnaud.claudel@simap.grenoble-inp.fr (A. Claudel).

work, a high temperature CVD process is explored to achieve high growth rate and high quality thick layers and later AlN single crystal bulk growth.

2. Thermodynamic analysis

Complex equilibria thermodynamic analysis of AlN HTCVD process was carried out using a procedure based on minimization of the whole Gibbs energy [38] with Factsage TM© using SGTE [39] and FACT [40] thermodynamic databases. Let us note that thermodynamic data for the condensed phase ⟨AlN⟩ are extrapolated when $T > 930\,^{\circ}C$ [41].

Our AlN HTCVD process consists in two steps. The first step is the synthesis of aluminum chlorides via the *in situ* reaction between Cl_2 and Al (chlorination reaction). The second step is the deposition step which correspond to the chemical reaction between $AlCl_x$ species and NH_3 with either H_2 or Ar as carrier gas.

Fig. 1 shows the effect of temperature at $P = 10^{-2}$ atm (a) and pressure at $T = 650\,^{\circ}C$ (b) on the formation of different $AlCl_x$ species by reaction between Al and Cl_2. It appears that equilibrium partial pressure of $AlCl_3$ is larger than that of AlCl below 790 °C and that AlCl and $AlCl_2$ only exist at high temperature above 500 °C (Fig. 1(a)). Concerning the effect of total pressure (Fig. 1(b)), the increasing of $AlCl_3$ and $AlCl_2$ partial pressures is similar while the Al_2Cl_6/AlCl ratio exhibits a strong increase with a crossover at about 0.2 atm. This thermodynamic study of Al chlorination by Cl_2 is in agreement with previous thermodynamic calculations of reaction between Al and HCl [17,18].

Such thermodynamic calculations indicate that $AlCl_x$ species formed by chlorination remain stable between 500 and 1500 °C. Above 1500 °C, $AlCl_3$ partial pressure decreases rapidly while AlCl (and $AlCl_2$) partial pressure increases. Fig. 2 shows the thermodynamic study of homogeneous reactions in the gas phase (starting from $AlCl_x$ synthesis at $T = 650\,^{\circ}C$, NH_3, H_2, Ar and without formation of any condensed phase). This indicates that AlCl plays an important role at high temperature above 1100 °C. Above 1200 °C, $AlCl_3$ partial pressure decreases while those of AlCl and $AlCl_2$ increase. AlCl partial pressure becomes larger than that of $AlCl_3$ above 1450 °C. Al_2Cl_6 and $AlCl_2H$ partial pressures decrease rapidly whereas those of $AlCl_2$ and Al (gas) increase strongly at high temperature. But these other Al-reactants are negligible (less than 1%). So, $AlCl_3$ and AlCl seem to be the most important Al sources in HTCVD process at low temperature (above 500 °C) and high temperature (above 1500 °C), respectively. H_2 remains stable but decreases slowly at high temperature to the advantage of H, HCl and also Cl which increase strongly with increasing temperature. H and Cl appear only above 1100 °C. NH_3 partial pressure is very low and does not appear in Fig. 2. Thermodynamically, NH_3 is rapidly dissociated in N_2 and H_2 when the temperature increases ($P_{NH_3} \approx 10^{-9}$ atm at 300 °C). In these calculations, NH_3 thermal dissociation is not inhibited so N_2 seems to be the only one N-reactant of this process which is not in good agreement with N_2 actual high thermal stability. But it is well known that NH_3 dissociation is catalyzed by metals and hindered by ceramicslike quartz (SiO_2) [42]. Furthermore, in previous thermodynamic studies, NH_3 dissociation was sometimes not considered because of this kinetic aspect [42] or of the formation of an adduct compound in gas phase such as $AlCl_3.NH_3$ [12,41–43] or Cl_2AlNH_2 [44,45]. To

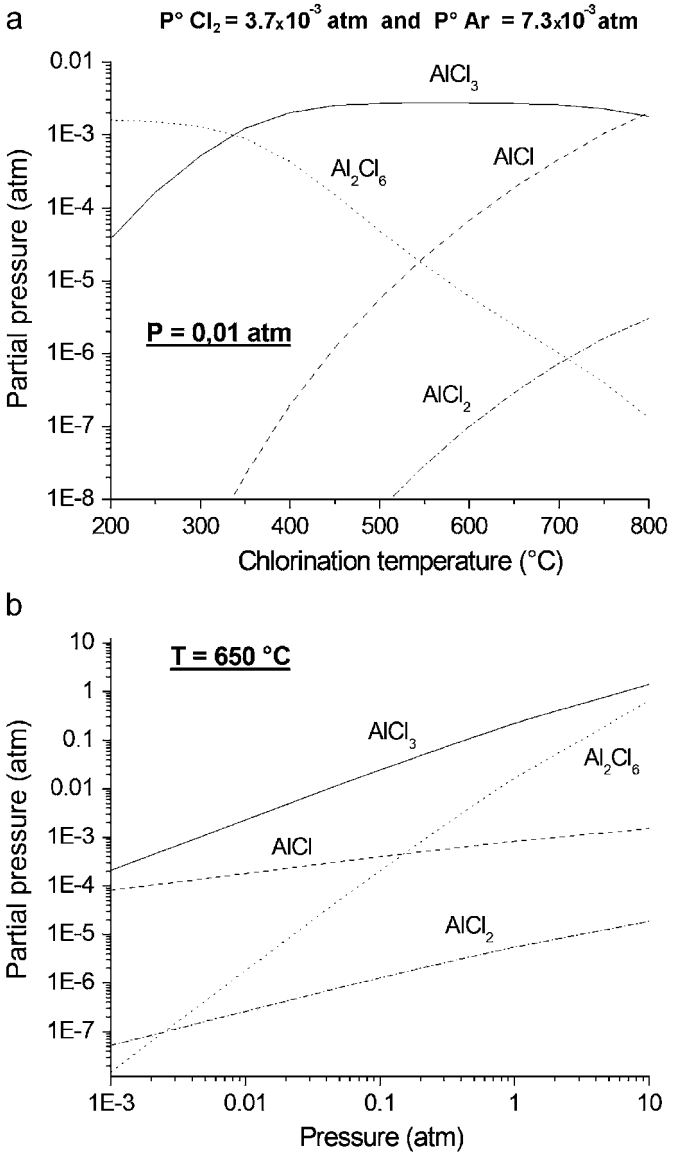

Fig. 1. Thermodynamic calculations on $AlCl_x$ partial pressures vs. temperature at 10^{-2} atm (a) and total pressure at 650 °C (b).

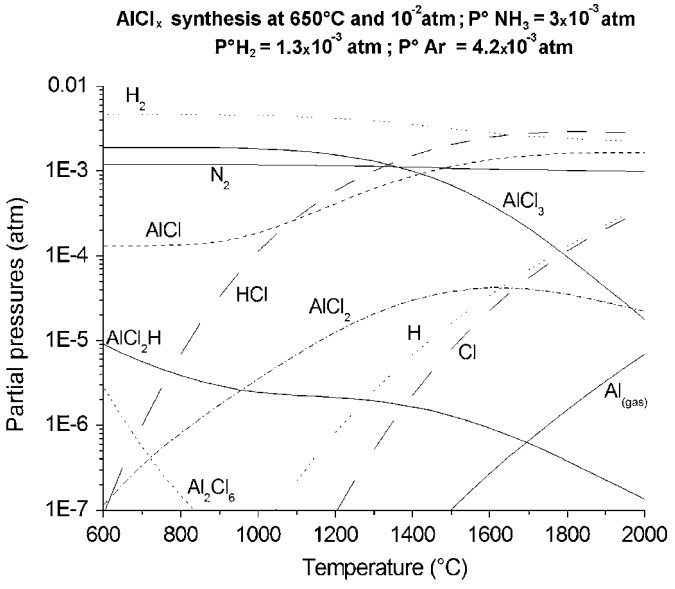

Fig. 2. Thermodynamic study of homogeneous reactions in the gas phase between 600 and 2000 °C ($P = 10^{-2}$ atm).

conclude on this point, kinetically, NH_3 (and perhaps NH_2 or NH at high temperature) seems to be the most important N source of AlN HTCVD.

The contribution of AlCl and $AlCl_3$ on AlN deposition step between 600 and 2000 °C was also studied in N_2 or NH_3 atmosphere starting from the four following equations:

$$3AlCl + N_2 \rightleftharpoons 2\langle AlN\rangle + AlCl_3 \quad (1)$$

$$2AlCl_3 + N_2 \rightleftharpoons 2\langle AlN\rangle + 3Cl_2 \quad (2)$$

$$AlCl + NH_3 \rightleftharpoons \langle AlN\rangle + HCl + H_2 \quad (3)$$

$$AlCl_3 + NH_3 \rightleftharpoons \langle AlN\rangle + 3HCl \quad (4)$$

Thermodynamic AlN deposition yield η was calculated with the following formula:

$$\eta = \frac{n\langle AlN\rangle}{\sum nAlCl_{x\ initial}} \times 100 \quad (5)$$

Using N_2 as N source, AlN synthesis cannot be realized with only $AlCl_3$ (Eq. (2)) but is thermodynamically possible with AlCl (Eq. (1)). In the second case, both AlCl and $AlCl_3$ can react with NH_3 to form AlN (Eqs. (3) and (4)) which shows the great importance of H in this CVD process. Results of our thermodynamic calculations indicate that in both cases the use of a AlCl–$AlCl_3$ mixture improves AlN deposition yield than $AlCl_3$ alone. AlN deposition from $AlCl_3$ and NH_3 decreases near 1200 °C and seems to be impossible above 1300 °C without AlCl. With AlCl species, AlN deposition is thermodynamically possible until 1600 °C. The decrease of AlN deposition at high temperature is due to the formation of the $AlCl + 2HCl + \frac{1}{2}N_2 + \frac{1}{2}H_2$ gas mixture, which is the most stable combination for gaseous species at high temperature [44,46]. However, in our experiments, AlN deposition was realized until 1800 °C which contradicts the thermodynamic impossibility on AlN growth above 1600 °C. An explanation could be that experimental thermodynamic data on AlN above 930 °C [41] and other compounds such as $AlCl_3.NH_3$ [12,42,43] are not available. Furthermore, the existence of a Cl_2AlNH_2 species which is also not included in these calculations is supposed by ab-initio calculations above 600–700 °C [44] and by analogy with Cl_2BNH_2 [45,47–49] (coming from direct reaction in gas phase between BCl_3 and NH_3) which was measured by HT mass spectrometry measurements in CVD conditions and seems to be a key species in BN deposition process [50,51].

Fig. 3(a) shows AlN deposition yield as a function of $AlCl_3$ and NH_3 partial pressures at 1100 °C and 10^{-2} atm. The maximum AlN deposition yield is found for a low $AlCl_3$ partial pressure and a high NH_3 partial pressure. Fig. 3(b) shows AlN deposition yield as a function of $AlCl_3$ and H_2 partial pressures at 1100 °C and 10^{-2} atm. AlN yield increases with increasing H_2 partial pressure at constant $AlCl_3$ and NH_3 partial pressures. Thermodynamically, the use of H_2 carrier gas promotes the formation of AlN compared to an inert gas such as Ar.

The influence of a variation to thermodynamic equilibrium defined as gas phase supersaturation was also studied. Experimentally, a variation of supersaturation in gas phase is known to have a great effect on surface morphology and crystallographic orientation of deposits. Usually, the epitaxial growth is favored with a low supersaturation [52,53]. In the case of AlN a low supersaturation is obtained at high temperature and for partial pressures of reactants near the thermodynamic equilibrium. In the present investigations, supersaturation α was calculated with the following formula:

$$\alpha = \frac{P_{Al\ species} \times P_{N\ species}}{P_{eq\,Al\ species} \times P_{eq\,N\ species}} \quad (6)$$

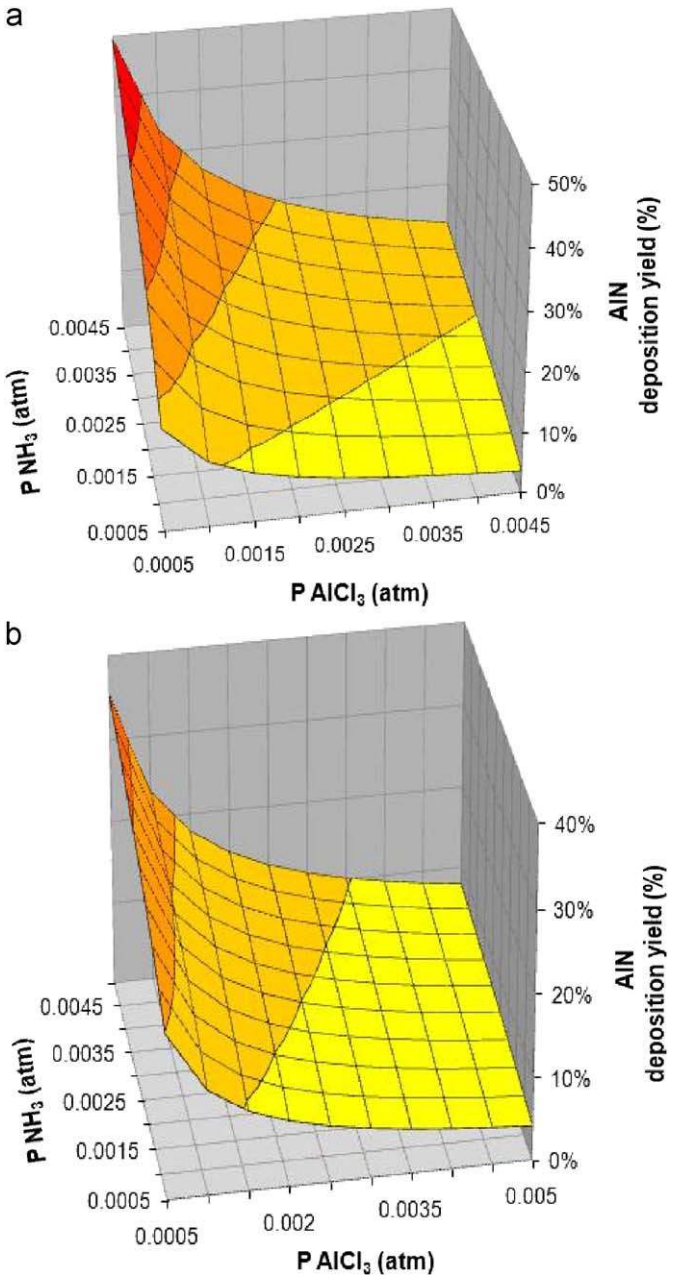

Fig. 3. AlN deposition yield vs. $AlCl_3$ and NH_3 partial pressures (a) and $AlCl_3$ and H_2 partial pressures (b) at $T = 1100$ °C and $P = 10^{-2}$ atm.

where P is the partial pressure of reactant species and P_{eq} is the calculated thermodynamic equilibrium partial pressure of Al and N species over solid AlN at given temperature and total pressure.

Fig. 4 shows calculated gas phase supersaturation α between 1000 and 2000 °C at 10^{-2} atm with different $H_2/AlCl_3$ ratio at a constant NH_3 partial pressure. Supersaturation decreases rapidly with increasing temperature and slowly with increasing $H_2/AlCl_3$ ratio.

Our thermodynamic calculations indicate that AlCl is a necessary precursor to grow AlN at high temperature with high growth rate, it is also known that AlCl is very reactive with quartz (SiO_2) reactor and this reaction is accelerated in the presence of H_2 [11]. For this reason, $AlCl_3$ is generally favored and generated by decreasing the temperature of the chloride source at 500 °C [17,18,20,21,23,24,27,28]. In our case, a water-cooled quartz tube (and a reactants dilution) prevent the reaction of AlCl with quartz.

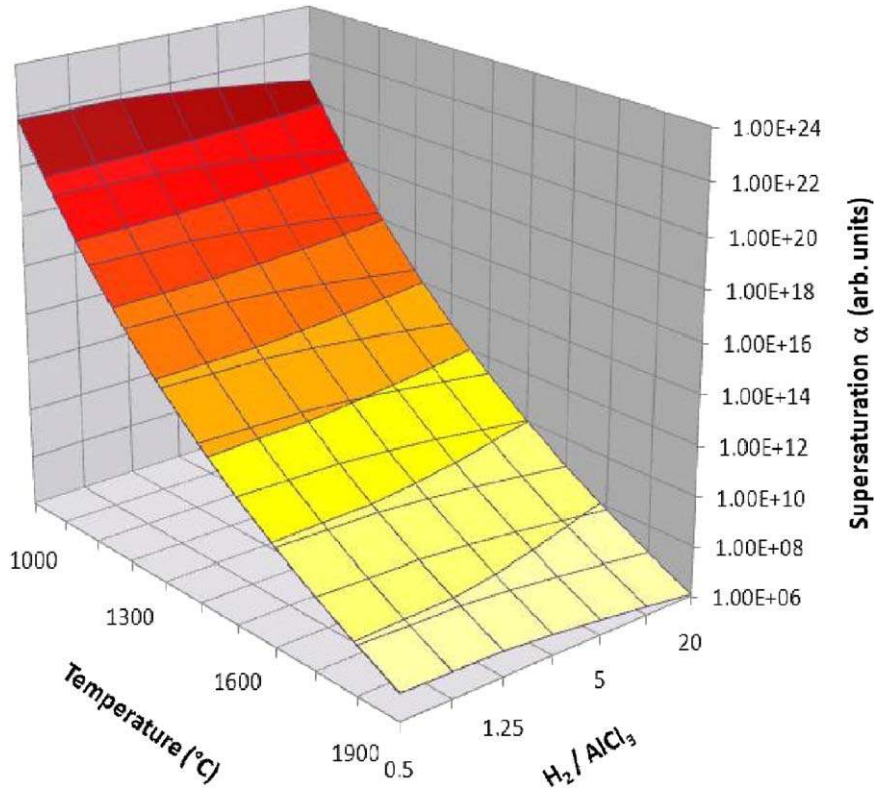

Fig. 4. Influence of temperature and $H_2/AlCl_3$ ratio on calculated supersaturation α (constant NH_3 partial pressure).

Based on these thermodynamic calculations of $AlCl_x$ synthesis and AlN deposition step, it is possible to grow AlN by HTCVD at low pressure in a water-cooled quartz reactor.

3. Experimental procedure

A schematic diagram of the HTCVD apparatus is shown in Fig. 5. The HTCVD set-up consists in a home-built vertical cold-wall reactor composed of two reaction zones [35,54]. The first one is the chlorination area where aluminum chlorides are generated via *in situ* reaction at 640 °C ($T_{melt.}$ Al = 660 °C) between Cl_2 and high purity Al wire contained in an inner tube heated by a lamp furnace. Then, $AlCl_x$ species are mixed with NH_3 and either H_2 or Ar as carrier gas. The second zone whose walls are water-cooled is the AlN deposition area. The substrate is located on top of a graphite susceptor heated by induction and the deposition temperature is measured on the graphite surface using InfraRed pyrometry. The NH_3 flow is in a (20–100 sccm) range and diluted in 200–1000 sccm of Ar or H_2. The Cl_2 flow rate is fixed between 2.5 and 100 sccm and diluted with Ar.

AlN films were deposited at low pressure on (0 0 0 1) α-Al_2O_3 Sapphire and (0 0 0 1) off axis 4H SiC or on axis 6H SiC single crystals between 1100 and 1800 °C. Let us note that a reaction occurs between Al_2O_3 and C above 1500 °C which induces the formation of CO, Al_2O and Al gases in agreement with our thermodynamic calculations and a previous study of the Al–C–O ternary system [55]. Before AlN deposition, Sapphire and SiC substrates were chemically etched in a HF 5% solution for 10 min. A thermal cleaning under H_2 atmosphere was also carried out above 1000 °C for 15 min. As-grown AlN layers surface morphologies were studied by SEM, FEG-SEM and AFM. Crystalline state, crystallographic orientations and epitaxial relationships with substrates were obtained from $\theta/2\theta$ X-ray diffraction and X-ray pole figure, respectively.

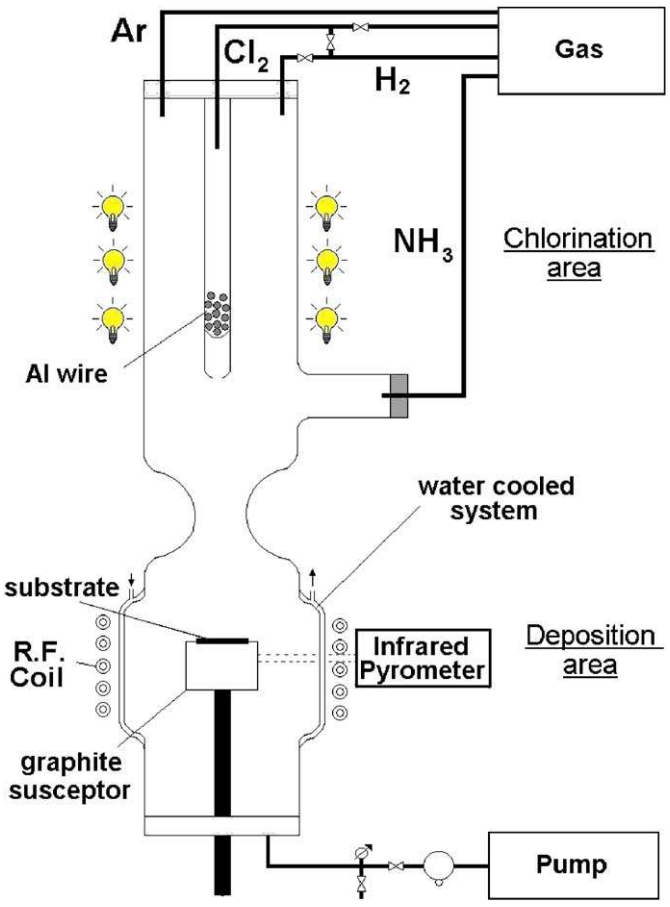

Fig. 5. High temperature CVD quartz reactor.

4. Results and discussions

In this experimental investigation, AlN films were deposited at different temperatures, in a range of 1100–1800 °C on different single crystal substrates: (0 0 0 1) Al_2O_3, (0 0 0 1) off axis 4H SiC and on axis 6H SiC [35]. Different conditions were tested in order to reach epitaxial growth. The influence of growth temperature, total pressure and chlorine flow rate were studied. Films morphology is also related to a variation of the thermodynamic supersaturation. Crack-free polycrystalline AlN layers were obtained with a thickness up to 150 μm and growth rates up to 200 μm h^{-1}. Their color varied from white to yellow and to brown with increasing Cl_2 flow rate. Yellow and brown colors of deposits seem to be related to an enrichment by aluminum in AlN interstitial sites [3,11,12]. Mirror-like AlN layers were grown up to a thickness of 30 μm but exhibited cracks. Any chlorine has not been found from X-EDS in all fabricated AlN films.

Fig. 6(a) is the typical kinetic curve which shows the variation of AlN growth rate on 4H SiC substrates as a function of the inverse of temperature in the 1100–1800 °C range at $P = 10$ Torr. Growth rate varied from 10 to 30 μm h^{-1}. At low temperature, this curve represents the kinetic regime of AlN deposition. High growth rates are obtained at high temperature which correspond to the diffusion regime [52]. A slight drop of deposition rate is observed at very high temperature and probably corresponds to the decrease of thermodynamic supersaturation (Fig. 4) and/or the beginning of powder formation by homogeneous nucleation in the gas phase [52,56–58]. Contrary to thermodynamic prediction, we definitely observed the formation of condensed AlN above 1600 °C. A new further assessment of thermodynamic data on the whole Al–N–H–Cl system at high temperature should be achieved as for the Si–C–H–Cl system [53,59–61]. Fig. 6(b) shows the variation of AlN growth rate as a function of total pressure at 1750 °C. AlN deposition rate decreases with increasing pressure between 10 and 100 Torr as previously reported by Suzuki and Tanji [58] but for a temperature of 1000 °C. Our thermodynamic analysis shows that AlN growth rate increases as a logarithmic function with increasing total pressure. The experimental trend cannot be explained by a thermodynamic approach but probably by chemical reactions, kinetic, gas dynamics and/or reactor's design effects. Fig. 6(c) shows the variation of AlN growth rate as a function of Cl_2 flow rate at 1750 °C and 10 Torr. Growth rate increases linearly with increasing Cl_2 flow rate which is in agreement with our thermodynamic calculations. So, in these conditions, the deposition of AlN is probably limited by the formation of $AlCl_x$ species, in agreement with previous investigations based on CVD using $AlCl_3$ [9,46,58] and on hydride vapor phase epitaxy using the reaction between HCl and Al [20,21,24,28].

The effect of carrier gas (Ar and/or H_2) was also studied. The use of H_2 as carrier gas allows to obtain higher growth rate as expected from thermodynamic calculations, more dense deposits and smoothest surface morphology than Ar. But it is still unclear if it comes from a chemical or a thermal effect.

Fig. 7 shows an X-ray diffraction pattern of preferred oriented (0 0 0 1) 2H AlN film deposited on (0 0 0 1) Sapphire substrate. From $\theta/2\theta$ scans related to diffracting vectors normal to the (0 0 0 1) surface of α-Al_2O_3 single crystal substrate, it has been deduced that each AlN sample exhibits a simple crystallographic orientational relationship with the substrate; i.e. $(0\,0\,0\,1)_{AlN}//(0\,0\,0\,1)_{\alpha\text{-}Al_2O_3}$ (Fig. 7(a)). Let us recall that both the structure AlN and α-Al_2O_3 are hexagonal $P6_3mc$ ($a = 3.1114$ Å, $c = 4.9792$ Å) and trigonal $R-3c$ ($a = 4.7617$ Å, $c = 12.9947$ Å or $a = 4.7617$ Å and $\alpha = 55.3004°$ for rhombohedral axes), respectively. However, from systematic plots of $\log(I) = f(2\theta)$, it could also be deduced that part of AlN layers were polycrystalline

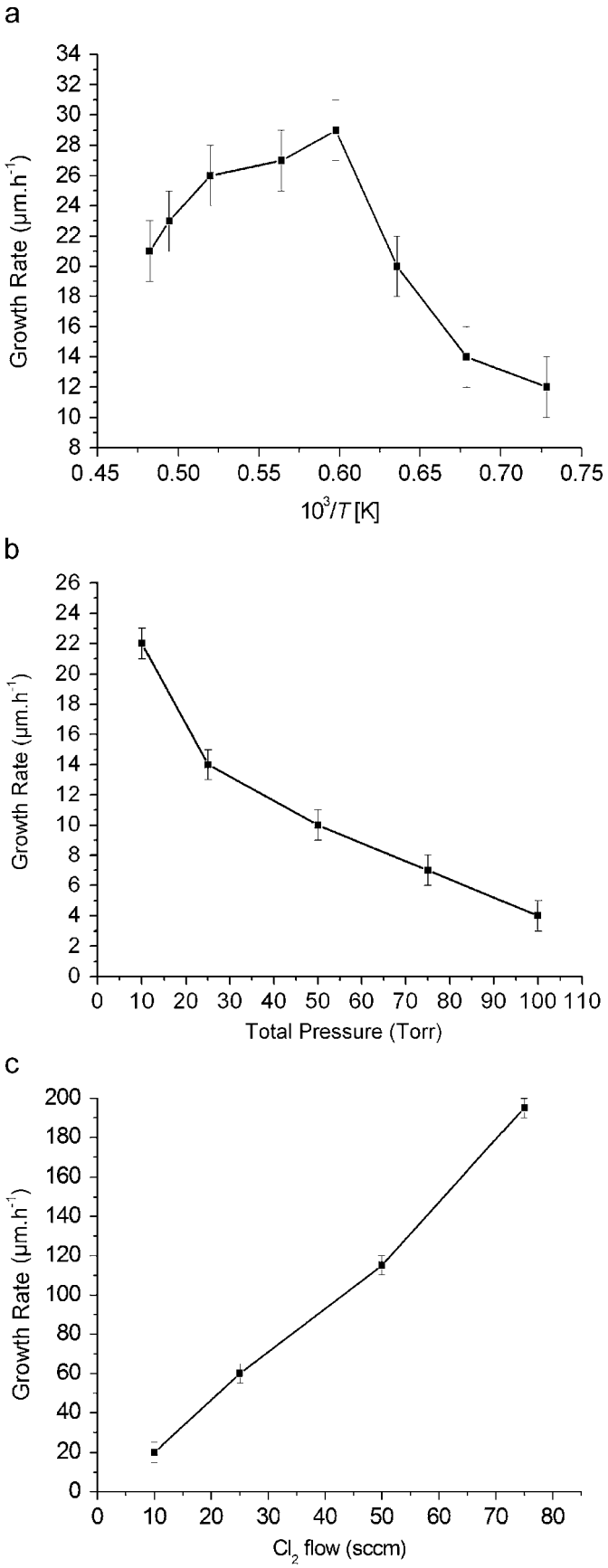

Fig. 6. Temperature (a), total pressure (b), and chlorine flow rate (c) effects on AlN growth rate on (0 0 0 1) 4H SiC substrates.

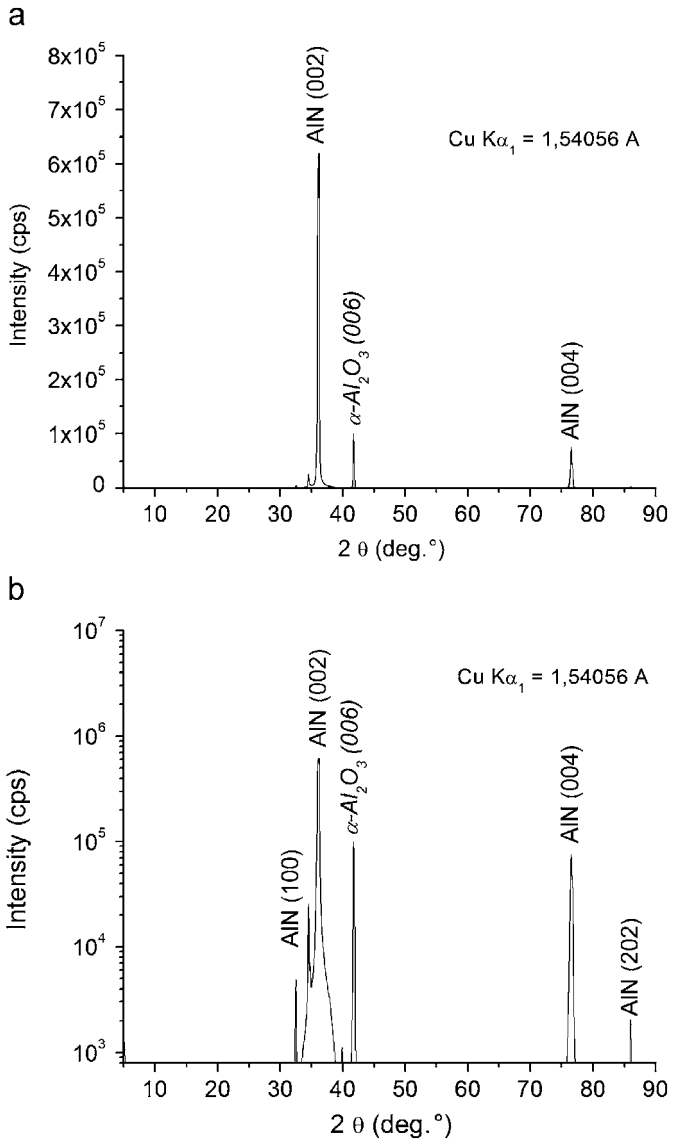

Fig. 7. Example of $\theta/2\theta$ X-ray diffraction pattern of an 2H AlN layer deposited on (0 0 0 1) Al_2O_3 single crystal substrate: (a) $I = f(2\theta)$ and (b) $\log(I) = f(2\theta)$.

(Fig. 7(b)). Same conclusions has been found for films deposited on 4H and 6H SiC single crystal substrates.

As the possibility of epitaxial relationships could be expected from the results of $\theta/2\theta$ X-ray diffraction, $\{1\,2\,\bar{3}\,3\}_{AlN}[0\,0\,0\,1]$ pole figures were determined using a texture goniometer in order to complete the characterization of crystallographic orientation of AlN layer with respect to its substrate, either (0 0 0 1) Al_2O_3 or (0 0 0 1) 4H SiC. Such X-ray diffraction measurements were performed around the [0 0 0 1] direction normal to the substrate up to a χ angle of 90°. The experimental results are represented on stereographic projections of [0 0 0 1] zone axis (Fig. 8). The $1\,2\,\bar{3}\,3$ reflections of AlN ($d_{1\,2\,\bar{3}\,3} = 0.868$ Å) being very close to the $4\,\bar{4}\,0\,8$ (or $0\,4\,4$) reflections of α-Al_2O_3, we have fixed a $\Delta\theta$ resolution of $\pm 0.14°$ in order to observe both these types of reflection from one φ, χ scan of 32,400 pointsonly. As a result, small intensities of $1\,2\,\bar{3}\,6_{4H\ SiC}$ and $1\,0\,\bar{1}\,1\,1_{4H\ SiC}$, also very close to $1\,2\,\bar{3}\,3_{AlN}$ reflections, are observed on these scans. The indexing of α-Al_2O_3 is related to rhombohedral axes which allows to identify the orientation of the threefold symmetry of this structure. The $0\,4\,4$ reflections of α-Al_2O_3 are represented by first order $0\,1\,1$ reflections as they project on same positions as $0\,4\,4$ reflections.

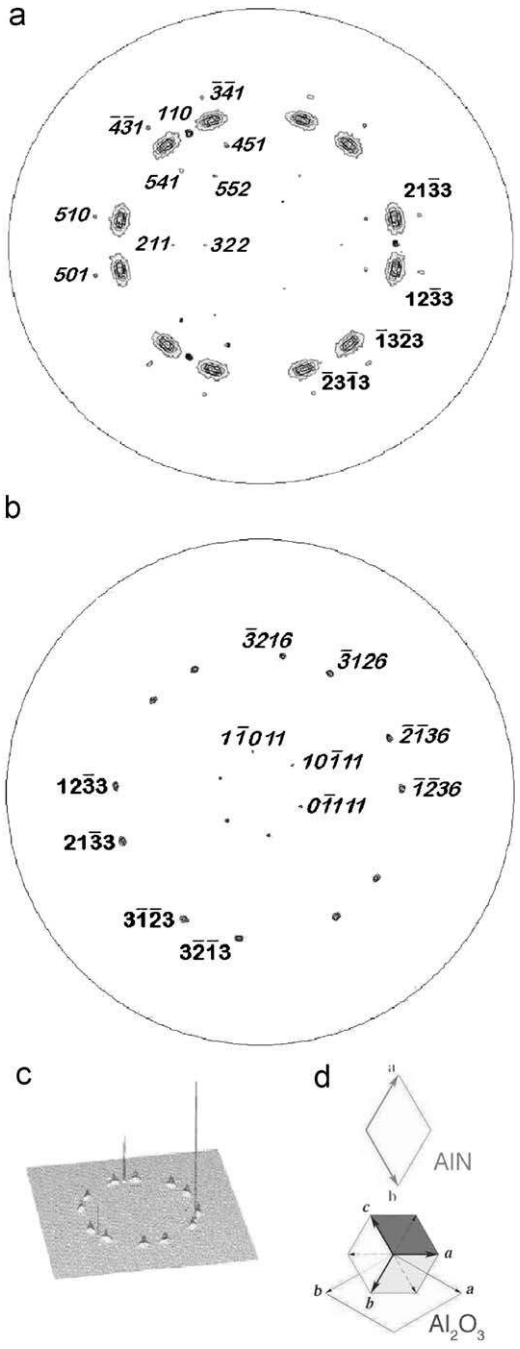

Fig. 8. Examples of $\{1\,2\,\bar{3}\,3\}_{AlN}$ [0 0 0 1] pole figures of AlN layers deposited on (0 0 0 1) Al_2O_3 (a) and (0 0 0 1) 4H SiC (b) performed up to a χ angle of 90° (in **bold** AlN reflexions, in *italic* Sapphire or 4H SiC substrate reflexions); in insert (c) plot indicating the relative intensity between $1\,2\,\bar{3}\,3_{AlN}$ and $0\,4\,4_{\alpha\text{-}Al_2O_3}$ reflections (d) the relative orientation of both AlN and α-Al_2O_3 cells.

Many other reflections of very weak intensity are also identified as corresponding to these of substrate α-Al_2O_3. Then it is straightforward to deduce from these pole figures the following epitaxial relationships:

$[0\,0\,0\,1]_{AlN}//[1\,1\,1]$ or $[0\,0\,0\,1]_{\alpha\text{-}Al_2O_3}$
$[1\,\bar{1}\,0\,0]_{AlN}//[\bar{1}\,0\,1]$ or $[1\,1\,\bar{2}\,0]_{\alpha\text{-}Al_2O_3}$
$[0\,0\,0\,1]_{AlN}//[0\,0\,0\,1]_{SiC}$
$[1\,\bar{1}\,0\,0]_{AlN}//[1\,\bar{1}\,0\,0]_{SiC}$

With increasing the temperature of HTCVD process, we have observed that the $1\,2\,\overline{3}\,3$ reflections of AlN become less broad and that the proportion of powder-like AlN diminishes.

The crystallinity of AlN layers in epitaxy on (0 0 0 1) off axis 4H SiC substrates was characterized using the ω scan method (rocking curves, RCs) [62,63]. X-ray rocking curves were measured on both 0 0 0 2 and $1\,0\,\overline{1}\,2$ AlN reflections in order to study out of plane (tilt) and in plane (twist) distortions, respectively. The lowest full-width at half-maximum (FWHM) values were 2100 arcsec (0.58°) for (0 0 0 2) and 1400 arcsec (0.39°) for $(1\,0\,\overline{1}\,2)$ in the case of a 10 μm AlN layer deposited in the following conditions: $T = 1750\,^{\circ}\mathrm{C}$, $P = 10$ Torr, low reactant flow rates and high carrier gas dilution. These values are important compared to those currently obtained on (0 0 0 1) on axis 6H SiC [25] or (0 0 0 1) Sapphire [31,33] and it is interesting to note that using this HTCVD process, tilt is more important than twist contrary to HVPE process [20,25,31,33].

Fig. 9 shows SEM images of AlN layers grown on 4H SiC substrates at various deposition temperatures with constant partial pressure of reactants and a total pressure of 10 Torr. With decreasing the supersaturation by increasing the deposition temperature, the surface morphologies obtained are sphere-like and become facetted and then smooth. So, rougher deposits are obtained at low temperature and smooth films at high deposition temperature. These smooth AlN layers obtained at high temperature were related to the AlN epitaxial growth from the previous $\theta/2\theta$ X-ray diffraction and X-ray pole figure experiments. However, several cracks were observed on such smooth AlN layers probably because of the difference of thermal expansion

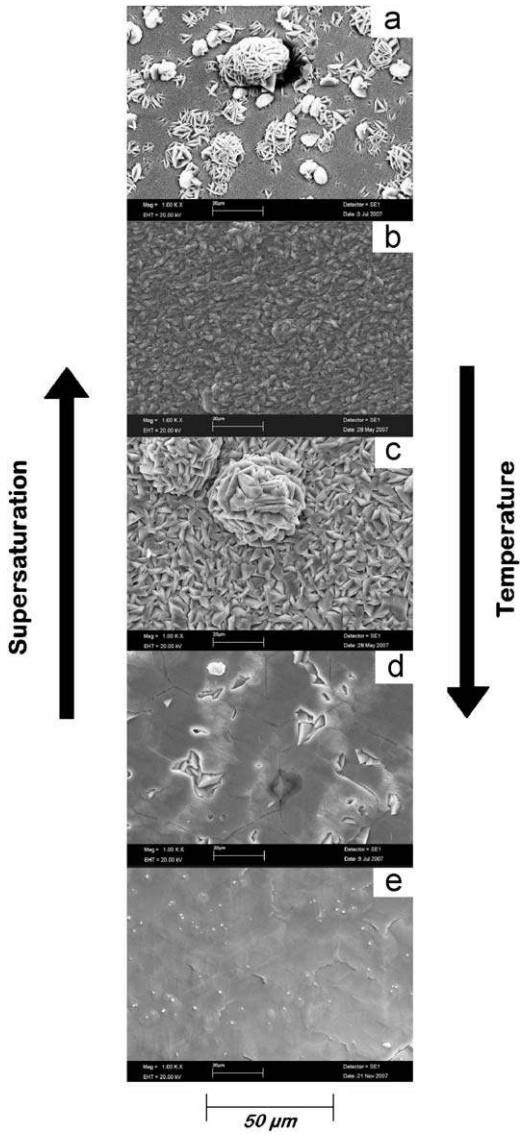

Fig. 9. SEM images of AlN layers grown on 4H SiC substrates at 1100 °C (a), 1300 °C (b), 1500 °C (c), 1650 °C (d) and 1750 °C (e) (constant reactants partial pressures and $P = 10$ Torr).

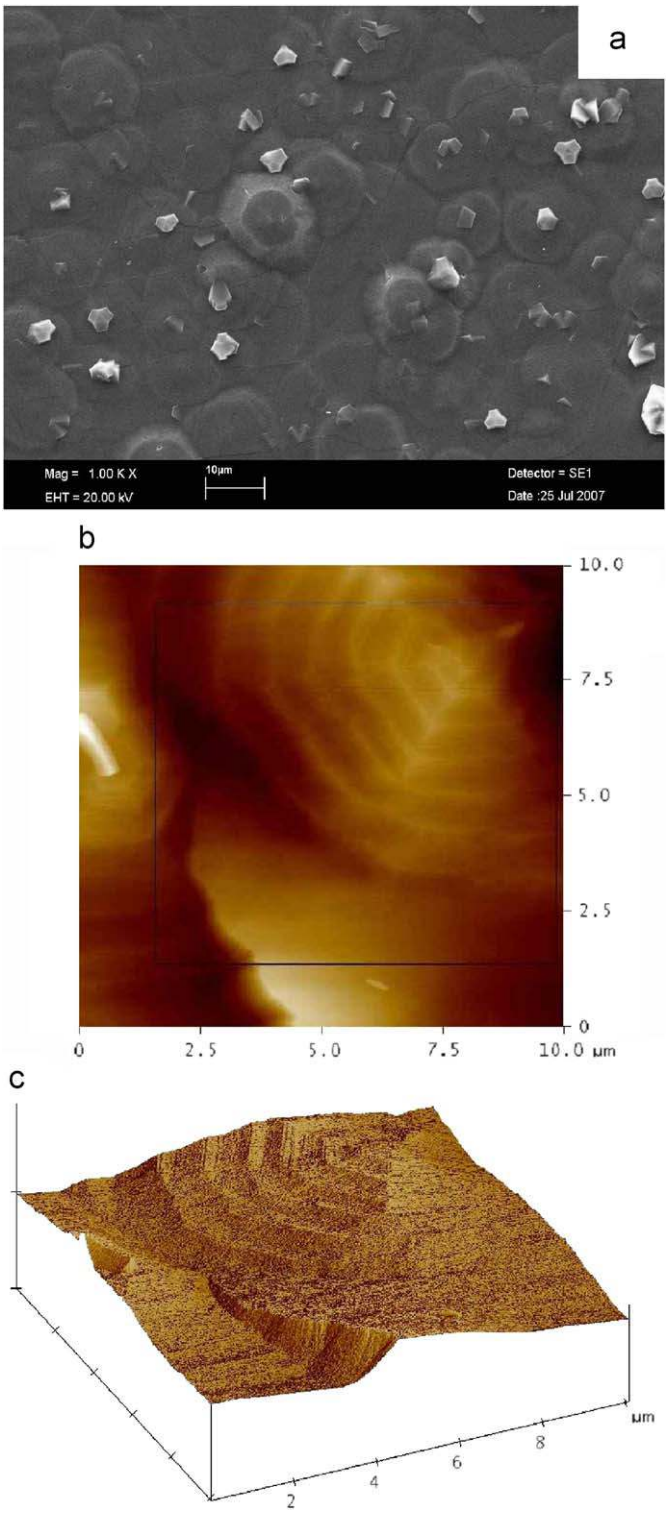

Fig. 10. SEM (a) and AFM ((b) and (c)) images of an AlN layer deposited at 1750 °C and 10 Torr on 6H SiC (on axis).

coefficient between AlN and the substrate at high temperature, lattice mismatch substrate-deposit and temperature ununiformity on the substrate surface.

Fig. 10 shows a SEM and AFM images of an AlN layer deposited at 1750 °C and 10 Torr on 6H SiC (on axis). This AlN layer exhibits hexagonal based hillocks (Fig. 10(a)). Those observed by AFM consist in polygonized spiral which very probably come from a preferential epitaxial growth around screw dislocations (Fig. 10(b) and (c)). Defect formation analysis, as done for SiC growth [64,65], should be very useful to understand the growth mechanisms. This growth mode is related to low supersaturation conditions and epitaxial growth. RMS roughness between 20 and 35 nm was obtained for such AlN layers.

5. Conclusions

Thermodynamic calculations on $AlCl_x$ synthesis and AlN deposition step indicate that it is possible to grow AlN by HTCVD at low pressure in a water-cooled quartz reactor. $AlCl_3$ and AlCl seem to be the most important Al-reactant in HTCVD process at low temperature and high temperature, respectively. However, several compounds formations by homogeneous reactions in gas phase and associated chemical mechanisms are still unclear. Experimentally, the growth of thick AlN layers on Sapphire and SiC substrates was achieved between 1100 and 1800 °C by HTCVD. Experiments prove that the use of H_2 as carrier gas instead of Ar allows to obtain higher growth rates, more dense deposits and smoothest surface morphologies. AlN epitaxial layers were grown when the deposition process was performed with low supersaturation conditions, i.e. high temperature and with partial pressures of reactants near the thermodynamic equilibrium. This epitaxial growth of AlN was also related to smooth surface morphology and exhibits hexagonal based hillocks related to a spiral growth around screw dislocations on axis 6H SiC. With increasing Cl_2 flow rate, AlN growth rate increases linearly and the epitaxial layer becomes polycrystalline with increasing deposition rate. The maximum growth rate of polycrystalline layers obtained at high temperature was about 200 $\mu m\,h^{-1}$. To conclude, HTCVD seems to be very promising for the development of a further bulk growth process to produce AlN single crystal substrates.

Acknowledgments

The authors wish to thank H. Roussel for X-ray diffraction experiments, G. Berthome for AFM characterizations and D. De Barros for help in CVD instrumentation.

This work was supported by Acerde, the French Ministère de l'Enseignement Supérieur et de la Recherche and Ministère de l'Economie, des Finances et de l'Industrie.

References

[1] G.A. Slack, T.F. Mc Nelly, Journal of Crystal Growth 34 (1976) 263.
[2] G.A. Slack, T.F. Mc Nelly, Journal of Crystal Growth 42 (1977) 560.
[3] G.A. Cox, D.O. Cummins, K. Kawabe, R.H. Tredgold, Journal of Physical Chemistry of Solids 28 (1967) 543.
[4] T. Renner, Zeitschrift vur Anorganische und Allgemeine Chemie 298 (300) (1959) 22.
[5] T.L. Chu, D.W. Ing, A.J. Noreika, Solid-State Electronics 10 (1967) 1023.
[6] A.J. Noreika, D.W. Ing, Journal of Applied Physics 39 (12) (1968) 5578.
[7] D.W. Lewis, Journal of the Electrochemical Society 117 (7) (1970) 978.
[8] T.L. Chu, R.W. Kelm Jr., Journal of Electrochemical Society 122 (1975) 995.
[9] J. Bauer, L. Biste, D. Bolze, Physica Status Solidi (A) 39 (1977) 173.
[10] W.M. Yim, E.J. Stofko, P.J. Zanzucchi, J.I. Pankove, M. Ettenberg, S.L. Gilbert, Journal of Applied Physics 44 (1) (1973) 292.
[11] M.P. Callaghan, E. Patterson, B.P. Richards, C.A. Wallace, Journal of Crystal Growth 22 (1974) 85.
[12] F. Bugge, A.F. Efimov, I.G. Pichugin, A.M. Tsaregorodtsev, M.A. Chernov, Crystal Research Technology 22 (1) (1987) 65.
[13] A. Nikolaev, I. Nikitina, A. Zubrilov, M. Mynbaeva, Y. Melnik, V. Dmitriev, Materials Research Society Symposium Proceedings (GaN and Related Alloys—1999), 2000, pp.595–598.
[14] V. Williams, E. Pernot, E. Ramberg, E. Blanquet, J.M. Bluet, R. Madar, Material Science Forum: Silicon Carbide and Related Materials 1999 (Part II) 338–342 (2000) 1507.
[15] Y. Melnik, D. Tsvetkov, A. Pechnikov, I. Nikitina, N. Kuznetsov, V. Dmitriev, Physica Status Solidi (A) 188 (1) (2001) 463.
[16] O.Y. Ledyaev, A.E. Cherenkov, A.E. Nikolaev, I.P. Nikitina, N.I. Kuznetsov, M.S. Dunaevski, A.N. Titkov, V.A. Dmitriev, Physica Status Solidi (C) 0 (1) (2002) 474.
[17] Y. Kumagai, H. Shikauchi, J. Kikuchi, T. Yamane, Y. Kangawa, A. Koukitu, in: Proceedings of 21st Century COE Joint Workshop on Bulk Nitrides IPAP Conferences Series, vol. 4, 2003, p.9.
[18] Y. Kumagai, T. Yamane, T. Miyaji, H. Murakami, Y. Kangawa, A. Koukitu, Physica Status Solidi (C) 7 (2003) 2498.
[19] Y. Melnik, Y. Soukhoveev, V. Ivantsov, V. Sivov, A. Pechnikov, K. Tsvetkov, O. Kovalenkov, V. Dmitriev, A. Nikolaev, N. Kuznetsov, E. Silveira, J. Freitas Jr., Physica Status Solidi (A) 200 (1) (2003) 22.
[20] Y. Kumagai, T. Yamane, A. Koukitu, Journal of Crystal Growth 281 (2005) 62.
[21] T. Yamane, H. Murakami, Y. Kangawa, Y. Kumagai, A. Koukitu, Physica Status Solidi (C) 7 (2005) 2062.
[22] O. Kovalenkov, V. Soukhoveev, V. Ivantsov, A. Usikov, V. Dmitriev, Journal of Crystal Growth 281 (2005) 87.
[23] Y.H. Liu, T. Tanabe, H. Miyake, K. Hiramatsu, T. Shibata, M. Tanaka, Y. Masa, Japanese Journal of Applied Physics (Letters) 44 (17) (2005) L505.
[24] Y. Kumagai, K. Takemoto, J. Kikuchi, T. Hasegawa, H. Murakami, A. Koukitu, Physica Status Solidi (B) 243 (7) (2006) 1431.
[25] V. Soukhoveev, O. Kovalenkov, V. Ivantsov, A. Syrkin, A. Usikov, V. Maslennikov, V. Dmitriev, Physica Status Solidi (C) 3 (6) (2006) 1653.
[26] V. Sukhoveev, A. Usikov, O. Kovalenkov, V. Ivantsov, A. Syrkin, V. Dmitriev, C. Collins, M. Wraback, Materials Research Society Symposium Proceedings 892 (29) (2006) 03.1.
[27] Y.-H. Liu, T. Tanabe, H. Miyake, K. Hiramatsu, T. Shibata, M. Tanaka, Journal of Physics: Condensed Matter 16 (2006) 1639.
[28] R.B. Jain, Y. Gao, J. Zhang, R.S. Qhaleed Fareed, R. Gaska, J. Li, A. Arjunan, E. Kuokstis, J. Yang, M. Asif Khan, Physica Status Solidi (C) 3 (6) (2006) 1491.
[29] T. Nagashima, M. Harada, H. Yanagi, Y. Kumagai, A. Koukitu, K. Takada, Journal of Crystal Growth 300 (2007) 42.
[30] K. Tsujisawa, S. Kishino, Y.H. Liu, M. Miyake, K. Hiramatsu, T. Shibata, M. Yanaka, Physica Status Solidi (C) 4 (7) (2007) 2252.
[31] T. Nagashima, M. Harada, H. Yanagi, H. Fukuyama, Y. Kumagai, A. Koukitu, K. Takada, Journal of Crystal Growth 305 (2007) 355.
[32] J. Tajima, Y. Kubota, R. Togashi, H. Murakami, Y. Kumagai, A. Koukitu, Physica Status Solidi (C) 5 (6) (2008) 1515.
[33] K.I. Eriguchi, T. Hiratsuka, H. Murakami, Y. Kumagai, A. Koukitu, Journal of Crystal Growth 310 (2008) 4016.
[34] Y. Kumagai, J. Tajima, M. Ishizuki, T. Nagashima, H. Murakami, K. Takada, A. Koukitu, Applied Physics Express 1 (2008) 045003.
[35] A. Claudel, E. Blanquet, D. Chaussende, M. Audier, D. Pique, M. Pons, Material Science Forum: Silicon Carbide and Related Materials 2007 600–603 (2009) 1269.
[36] M.T. Duffy, C.C. Wang, G.D. O'Clock Jr., S.H. McFarlane III, P.J. Zanzucchi, Journal of Electronic Materials 2 (2) (1972) 359.
[37] M. Morita, N. Uesugi, S. Isogal, K. Tsubouchi, N. Mikoshiba, Japanese Journal of Applied Physics 20 (1) (1981) 17.
[38] C. Bernard, E. Blanquet, M. Pons, Surface and Coating Technology 202 (4–7) (2007) 790.
[39] SGTE, Institut National Polytechnique de Grenoble (LTPCM), Grenoble, France, ⟨http://www.sgte.org⟩.
[40] FactSage, ⟨http://www.factsage.com⟩.
[41] I.N. Przhevalskii, S.Y. Karpov, Y.N. Makarov, MRS Internet Journal of Nitride Semiconductor Research 3 (1998) 30.
[42] K.G. Nickel, R. Riedel, G. Petzow, Journal of American Ceramic Society 72 (10) (1989) 1804.
[43] H. Arnold, L. Bister, T. Kaufmann, Kristall und Technik 13 (8) (1978) 929.
[44] A.Y. Timoshkin, H.F. Bettinger, H.F. Schaefer, Journal of the American Chemical Society 119 (1997) 5668.
[45] A. Dollet, Y. Casaux, R. Rodriguez-Clemente, Proceedings—Electrochemical Society (Chemical Vapor Deposition) 97 (25) (1997) 286.
[46] W.Y. Lee, W.J. Lackey, P.K. Agrawal, Journal of the American Ceramic Society 74 (1991) 1821.
[47] A. Dollet, Y. Casaux, M. Mtecki, R. Rodriguez-Clemente, Thin Solid Films 406 (2002) 1.
[48] A. Dollet, Y. Casaux, M. Mtecki, R. Rodriguez-Clemente, Thin Solid Films 406 (2002) 118.
[49] D. Cai, L.L. Zheng, H. Zhang, V.L. Tassev, D.F. Bliss, Journal of Crystal Growth 276 (2005) 182.
[50] M.D. Allendorf, T.H. Osterheld, Proceedings—Electrochemical Society PV 96 (5) (1996) 16.
[51] A.H. Mc Daniel, M.D. Allendorf, Journal of Physical Chemistry A 102 (40) (1998) 7804.
[52] W.A. Bryant, Journal of Materials Science 12 (1977) 1285.

[53] G. Chichignoud, M. Ucar-Morais, P. Pons, E. Blanquet, Surface and Coating Technology 201 (22–23) (2007) 8888.
[54] E. Blanquet, C. Vahlas, R. Madar, J. Palleau, J. Torres, C. Bernard, Thin Solid Films 177 (1989) 189.
[55] M. Heyrman, G. Berthomé, A. Pisch, C. Chatillon, Journal of the Electrochemical Society 153 (10) (2006) J107.
[56] K.J. Sladek, Journal of the Electrochemical Society 118 (4) (1971) 654.
[57] M. Suzuki, H. Tanji, Proceedings—Electrochemical Society (Proceedings of International Conference on Chemcial Vapor Deposition, 10th) vol. 87 (8) (1987) 1089.
[58] T. Goto, J. Tsuneyoshi, K. Kaya, T. Hirai, Journal of Materials Science 27 (1992) 247.
[59] M.D. Allendorf, C.F. Melius, The Journal of Physical Chemistry 97 (3) (1993) 720.
[60] P. Rocabois, C. Chatillon, C. Bernard, High Temperatures—High Pressures 27/28 (1) (1996) 3.
[61] P. Rocabois, C. Chatillon, C. Bernard, F. Genet, High Temperatures—High Pressures 27/28 (1) (1996) 25.
[62] H. Mank, B. Amstatt, D. Turover, E. Bellet-Amalric, B. Daudin, V. Ivantsov, V. Dmitriev, V. Maslennikov, Physica Status Solidi (C) 3 (6) (2006) 1448.
[63] E. Bellet-Amalric, C. Adelmann, E. Sarigiannidou, J.L. Rouviere, G. Feuillet, E. Monroy, B. Daudin, Journal of Applied Physics 95 (2004) 1127.
[64] K. Chourou, M. Anikin, J.M. Bluet, J.M. Dedulle, R. Madar, M. Pons, E. Blanquet, C. Bernard, P. Grosse, C. Faure, G. Basset, Y. Grange, Materials Science and Engineering B 61–62 (1999) 82.
[65] R. Madar, M. Anikin, K. Chourou, M. Labeau, M. Pons, E. Blanquet, J.M. Dedulle, C. Bernard, S. Milita, J. Baruchel, Diamond and Related Materials 6 (1997) 1249.